www.lajss.org
Latin American Journal of Solids and Structures 5 (2008)237–258

Service load behavior of low rise composite frames considering creep, shrinkage and cracking

Sandeep Chaudhary[1], Umesh Pendharkar[2], A.K. Nagpal [3,*]

[1]Deptt. of Structural Engg., Malaviya National Institute of Technology, Jaipur, India.
[2]Deptt. of Civil Engg., Ujjain Engineering College, Ujjain, India.
[3]Professor Department of Civil Engineering, Indian Institute of Technology Delhi, Hauz Khas, New Delhi -110016, India. Tel: +91 11 26591234; Fax: + 91 11 26581117

Abstract

Composite beams with precast decks have an advantage in the speed of construction. Systematic studies are reported for the service load behavior of composite frames consisting of this type of composite beams and steel columns. A hybrid procedure recently developed by the authors, for the analysis of such composite frames subjected to service load, has been used for carrying out the studies. The applicability of the procedure has been demonstrated for composite construction with precast slabs and then detailed studies have been carried out for a single story frame. The age of concrete at the time of loading, magnitude of load, grade of concrete, relative humidity and tension stiffening are the parameters whose effects have been studied on the bending moments at the beam ends and midspan deflections. The relative humidity is found to be the more significant parameter affecting the time-dependent changes in bending moments and midspan deflections. Form the studies carried out for a five story and a eight story frame, it is shown that the use of simplified models (substitute frames) can lead to errors .

Keywords: Composite Frame, Cracking, Creep, Shrinkage, Service Load.

Notations

A, B, I= Area, first moment of area and second moment of area respectively;
E_c, E_s = Modulus of elasticity of concrete and steel respectively;
L = Span length;
M = Bending moment;
RH = Relative humidity;
d_m = Midspan deflection;
f_{ck} = Characteristic compressive strength of concrete;
f_t = Tensile strength of concrete;
f_{ij} = Flexibility coefficients;
t_1 = Age of concrete at time of loading;

*Corresp. author Email: aknagpal@civil.iitd.ernet.in Received 25 Feb 2008; In revised form 18 Aug 2008

t_s = Time duration of curing;
w = Uniformly distributed load;
x = Crack length;
y = $L - x$;
ϕ, ε^{sh} = Creep coefficient and shrinkage strain respectively;
ξ = Interpolation coefficient;
η = $1 - \xi$;

Subscript

A, B = Ends A and B respectively;
cr, un = Cracked state and uncracked state respectively;

Superscript

it, t = Instantaneous and total respectively;

1 Introduction

Composite frames, consisting of steel frame and concrete decks, are an economical form of construction. Further, the use of precast decks, in place of cast insitu concrete decks, has an advantage in the speed of construction. Recently, there has been an increasing use of such construction. In the composite frames subjected to service load, in addition to instantaneous cracking, the time-dependent effects of creep and shrinkage in concrete can lead to the progressive cracking of concrete deck near the beam ends and result in considerable moment redistribution along with increase in deflections of composite beams.

Extensive literature is available on the instantaneous and time-dependent behavior of the continuous composite beams (Figure 1). Dezi and Tarantino [7] carried out parametric studies on two span composite continuous beams. The effect of three rheological parameters i.e. compressive strength of concrete (f_{ck}), relative humidity (RH) and age of concrete at loading (t_1) was studied on the time-dependent behavior. The concrete was assumed to be uncracked. It was found that creep has more effect for low values of concrete age at loading, compressive strength of concrete and relative humidity. Virtuoso and Vieira [23] have studied the time-dependent behavior of two span continuous composite beams with flexible connection and concluded that the effect of creep simultaneously with shrinkage is more important than the effect of creep alone. It was also observed that due to creep and shrinkage of concrete slab, there is a transfer of stresses from concrete to steel which is lesser for flexible connections. In another study by Ranzi [19] carried out on the simply supported stiffened composite beams for the effect of relative humidity and compressive strength, the relative humidity was found to be the major factor influencing the time-dependent behavior. Some other studies [17,18] have also been reported for the time-dependent behavior of continuous composite beams. These studies are mainly related to the effect of construction sequence and, the overall effect of creep and shrinkage but not of the

individual rheological parameters is presented. Studies are also available on the time-dependent effects of precast prestressed concrete girder bridges [11, 22] in which the relative effect of creep and shrinkage [22] and of some rheological factors [11] has been presented.

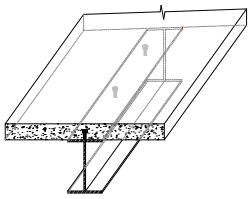

Figure 1: Isometric view of a composite beam.

In the above cited literature, the flexibility of shear connectors has been incorporated. It has been demonstrated by Ryu et al. [21] that the effect of flexibility of shear connections is negligible if the strength of shear connection is greater than the strength required for full shear connection.

In the regions where the tensile stress exceeds the tensile strength of the concrete, cracking occurs. The length of the cracked portion, along with the other factors, depends on the magnitude of load, . Owing to the distributed nature of cracking, the effective rigidity of the sections is higher than the rigidity of the cracked sections (tension stiffening effect). The displacements may be overestimated if this effect is neglected [12, 14].

No studies are available on the effect of individual parameters, i.e. t_1, w, f_{ck}, RH and tension stiffening on the service load behavior of the composite frames consisting of steel frames and precast decks. The present paper therefore reports systematic studies for the service load behavior of such composite frames. First, for a single story frame, the effect of the individual parameters has been studied on the bending moments and the midspan deflections of beams. Subsequently, for typical values of the parameters, studies have also been carried out for a five story and a eight story frame.

2 Hybrid procedure for analysis of composite frames

A recently developed hybrid analytical-numerical procedure [4–6] for the composite structures has been used for studying the behavior of composite frames. The procedure is highly computationally efficient and takes into account the non-linear effects of concrete cracking and time-dependent effects of creep and shrinkage in concrete portion of the composite beams. The procedure is analytical at the elemental level and numerical at the structural level. A cracked span length beam element consisting of an uncracked zone in the middle and cracked zones at the ends (Figure 2a,b) has been used in the procedure. Slip has been neglected by assuming a high degree of shear connection for which slip has little influence [21]. The concrete portion across the cross-section is assumed to be completely cracked, when the top stress of the concrete

slab exceeds the tensile strength of the concrete, f_t [13].

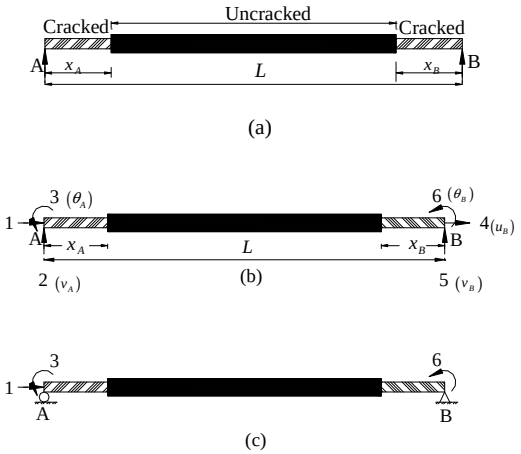

Figure 2: Cracked span length beam element: (a) zones; (b) degrees of freedom; and (c) releases 1, 3 and 6.

The frames are assumed to be subjected to service load and therefore concrete is assumed to be linear elastic in compression (assuming the compressive stresses do not exceed the 40% of the compressive strength) and in tension before cracking. The tension stiffening effect for the cracked zone is taken into account by considering the cross section in two states, cracked and uncracked. The cracked state is assumed to consist only of steel section and reinforcement in concrete slab and no creep and shrinkage is assumed to take place in the cracked state. The contribution of the cracked state is represented by interpolation coefficient,ξ whereas the contribution of the uncracked state is represented by $\eta(= 1 - \xi)$. The curvature, ρ_{ts} and strain, ε_{ts} in cracked zone are given as $\rho_{ts} = \eta\rho_{un} + \xi\rho_{cr}$ and $\varepsilon_{ts} = \eta\varepsilon_{un} + \xi\varepsilon_{cr}$ where ρ_{un}, ρ_{cr}=curvature of cross section assuming it to be completely uncracked and cracked respectively; ε_{un}, ε_{cr}=strain in the top fiber assuming the section to be completely uncracked and cracked respectively.

The interpolation coefficient is evaluated by the following expression, based on Eurocode 2 [8]

$$\xi = 1 - k(f_t/\sigma_{un})^2 \tag{1}$$

where k= a factor for reduction in tension stiffening with time and σ_{un}= the tensile stress in the top fiber.

Steel is assumed to be linear elastic in both tension and compression assuming the stresses to be below yield stress, this would generally be the case when high strength steel is used.

The analysis in the hybrid procedure is carried out in two parts. In the first part, instantaneous analysis is carried out using an iterative method. In the second part, time-dependent analysis is carried out by dividing the time into a number of time intervals to take into account

the progressive nature of cracking of concrete (Figure 3). For the instantaneous analysis, the value of k is assumed to be 1.0. For time-dependent analysis, considering the findings of Rutner [20], the value of k at any time instant is given as 0.65-0.15(ϕ/ϕ_u) where ϕ_u= the ultimate creep coefficient. The cracking and time-dependent effects of creep and shrinkage are therefore dependent on each other.

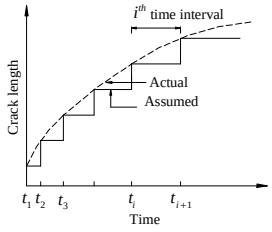

Figure 3: Actual and assumed progressive nature of cracking.

In the time-dependent analysis, crack length is assumed to be constant and equal to that at the beginning of the time-interval, as shown in Figure 3. The age-adjusted effective modulus method, AAEMM [1] is used for predicting the creep and shrinkage effects. Instead of conventional manner of application of AAEMM for one step, a number of time steps, as stated above, have been considered and the creep and shrinkage effects are evaluated for the revised crack lengths in each time interval.

Closed form expressions for flexibility coefficients, end displacements, crack lengths and midspan deflection of the cracked span length beam element have been used in order to reduce the computational efforts. The closed form expressions for the flexibility coefficients (w.r.t. releases 1, 3 and 6) of the typical span length beam element (Figure 2a, c) are given as [5]

$$f_{11} = [S^y_{un}(L - \xi_A x_A - \xi_B x_B + S^y_{cr}(\xi_A x_A + \xi_B x_B)] \tag{2}$$

$$f_{13} = f_{31} = \frac{1}{2L}\left[S^{xy}_{un}(\eta_A L^2 - \xi_B {x_B}^2 + \xi_A {y_A}^2) + S^{xy}_{cr}(\xi_A L^2 + \xi_B {x_B}^2 - \xi_A {y_A}^2)\right] \tag{3}$$

$$f_{16} = f_{61} = \frac{1}{2L}\left[S^{xy}_{un}(\eta_B L^2 - \xi_A {x_A}^2 + \xi_B {y_B}^2) + S^{xy}_{cr}(\xi_B L^2 + \xi_A {x_A}^2 - \xi_B {y_B}^2)\right] \tag{4}$$

$$f_{33} = \frac{1}{3L^2}\left[S^x_{un}(\eta_A L^3 - \xi_B {x_B}^3 + \xi_A {y_A}^3) + S^x_{cr}(\xi_A L^3 + \xi_B {x_B}^3 - \xi_A {y_A}^3)\right] \tag{5}$$

$$f_{36} = f_{63} = \frac{1}{6L^2}\left[\xi_A {x_A}^2(2x_A - 3L) + \xi_B {x_B}^2(2x_B - 3L)\right](S^x_{cr} - S^x_{un}) - \frac{S^x_{un} L}{6} \tag{6}$$

$$f_{66} = \frac{1}{3L^2}\left[S^x_{un}(\eta_B L^3 - \xi_A {x_A}^3 + \xi_B {y_B}^3) + S^x_{cr}(\xi_B L^3 + \xi_A {x_A}^3 - \xi_B {y_B}^3)\right] \tag{7}$$

where, ξ_A, ξ_B= interpolation coefficients for the cracked zones at ends A and B respectively to account for the tension stiffening effect; $\eta_A = 1 - \xi_A$; $\eta_B = 1 - \xi_B$; x_A, x_B= crack lengths at ends A and B respectively; $y_A = L - x_A$; $y_B = 1 - x_B$; and S^x, S^{xy} and S^y are given as

$$S^x = \frac{A}{E_c(AI - B^2)} \tag{8}$$

$$S^{xy} = \frac{B}{E_c(AI - B^2)} \tag{9}$$

$$S^y = \frac{I}{E_c(AI - B^2)} \tag{10}$$

where E_c= modulus of elasticity of concrete; A= area of the transformed cross-section and B, I = first and second moment of area of the transformed cross-section about the reference axis respectively. The quantities S^x_{un}, S^{xy}_{un} and S^y_{un} are evaluated using the uncracked state properties, whereas S^x_{cr}, S^{xy}_{cr} and S^y_{cr} are evaluated using the cracked state properties. It may be noted that the flexibility matrix coefficients f_{13}, f_{31}, f_{16} and f_{61}, are not zero because the reference axis is not at the centroid of the composite section. The coefficients of stiffness matrix, $[k]$ corresponding to d.o.f. 1, 3 and 6 are now obtained by inverting the flexibility matrix coefficients corresponding to d.o.f. 1, 3 and 6 (on using the readily available expressions for inversion of 3×3 matrix). Remaining terms corresponding to d.o.f. 2, 4 and 5 are obtained by applying the equilibrium conditions. Similarly, the closed form expressions for other quantities may be obtained from Chaudhary et al. [5].

This hybrid procedure [4–6] has been validated by comparison with the experimental and analytical results for two span continuous composite beams. Further, the procedure has also been validated with the FEM model for a composite frame using ABAQUS.

To verify the applicability of the procedure for composite construction with precast decks, the procedure has been validated for an overhanging simple support composite beam (beam EB1) of total 28 m length (length of overhang on each side =12.0 m) with precast concrete decks, for which experiments were conducted by Ryu et al. [21]. Equal magnitude of load was applied at both the left and right free ends. The shear connections of the beam were made fully rigid.

The beam has been modeled as a limiting case of a three bay single story frame in the hybrid procedure. The exterior supports are assumed to be completely released. One interior support is modeled as a hinge whereas the other interior support is modeled as roller. To achieve this, the interior columns are assumed to have a large area, negligible moment of inertia and negligible length whereas the exterior columns are assumed to have all the three quantities negligible.

The load-deflection variations at left and right free ends of beam EB1 obtained by the proposed procedure are compared with the experimental values reported by Ryu et al. [21] for the service load range i.e. the range in which yielding of steel may not take place.

The deflection obtained from the proposed procedure and the experimental values are shown in Figure 4. It may be noted that even though the transverse joints were found to be cracked earlier than the precast decks in the experiment, the results from the hybrid procedure which neglect the cracking of the transverse joints are in reasonable agreement with experimental results. This shows that the cracking of joints (the cumulative thickness of which is a very small portion of the beam length) has a small effect on the behavior of composite beams. The proposed procedure can therefore be applied for composite beams with precast concrete decks as well.

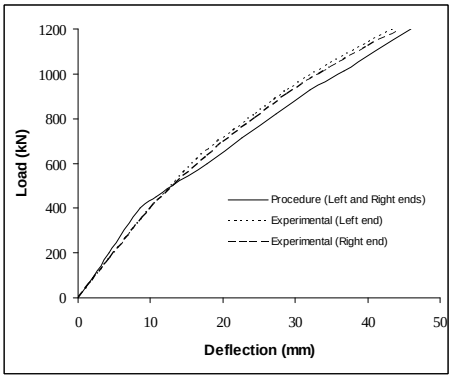

Figure 4: Load deflection variations for at left and right free ends of beam EB1.

3 Parametric Study

First a single story frame (Figure 5) is considered to study, in detail, the effect of t_1, w, f_{ck}, and tension stiffening. Then, two composite frames (Figure 6, number of story, n = 5 and 8) are considered for typical values of these parameters.

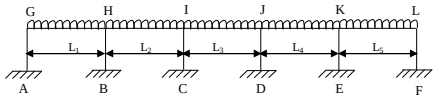

Figure 5: Frame EF1.

CEB-FIP MC90 [2] along with its update, *fib* [16] is used for predicting the properties of the concrete as well as the creep coefficients and shrinkage strains. The updated model is referred to as CEB-FIP MC90-99 in the paper. Cement is assumed to be of normal type and mean temperature is assumed to be 20 degree Celsius. Unless stated otherwise, a total time-duration of 20,000 days is considered and is divided into 20 time intervals to account for progressive cracking. Duration of time intervals is chosen such that an equal amount of shrinkage takes

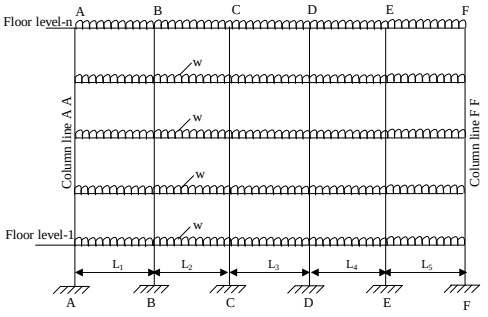

Figure 6: Frame EF2 and EF3.

place in each time interval [3, 5]. In these references it has been found that the number of time intervals required for convergence of values of moments and midspan deflections within 1% is less than 20. At the time of application of the load, instantaneous bending moments, $M^{it}(t_1)$ (in which, here and subsequently for other quantities having one term in the parentheses, the term indicates the time instant at which the quantity is evaluated or assumed to arise), and instantaneous midspan deflections, $d^{it}(t_1)$ are obtained by neglecting cracking (elastic values) and considering cracking (inelastic values). It may be noted that the inelastic values here and later on refer to the non linearity introduced by cracking of concrete only and does not refer to any other non linearity. For the time-dependent analysis $(t_1, t_2, ..., t_{21})$, total bending moments, $M^t(t)$ and total midspan deflections, $d^t(t)$ at time t are obtained by considering the cracked state at t_1 and subsequent progressive cracking.

3.1 Single Story Frame

A single story frame of five spans (Figure 4, $L_1 = L_2 = L_3 = L_4 = L_5$=7.0m) is considered. The columns of the frame are of the steel section (203×102 UB 23). The cross-section of the composite beams (beams GH, HI, IJ, JK and KL) consists of a steel section (356×171 UB 67) and precast concrete slabs of cross-section 1100 mm×75 mm with a reinforcement of area 508 mm^2 placed at a distance of 15 mm from the top fiber. The beams of the frame have been designed according to Eurocode 4 [9] and the columns have been designed according to Eurocode 3 [10], for a load of 30 kN/m acting on the beams. The construction is assumed to be propped with the props assumed to be removed, on the formation of the composite section. It is also assumed that the load gets applied at the same time and is resisted by the composite section.

The studies for this frame are first reported for the four parameters $(t_1, w, f_{ck}$, RH) by varying each of the parameters in turn and keeping other three parameters constant. Tension stiffening is included in these studies. Then, the effect of tension stiffening is studied keeping the other parameters constant. It may be noted that the compressive strength of concrete (grade of concrete) and the relative humidity have been identified as the two most important parameters affecting creep and shrinkage for concrete specimens by Howells et al. [15].

Table 1: Effect of age at loading on instantaneous and total bending moments at ends of beams of frame EF1 for w=20.00 kN/m,f_{ck}=30N/mm^{2}and RH=70%.

Beam	**End**	**Age (Days)**	**Bending Moment (kNm)**				**Time-dependent % change**	
			Instantaneous, $M^{it}(t_1)$		**Total,** $M^t(t_{21})$			
			Elastic (No Cracking)	Inelastic (Cracking)	Creep only	Creep & shrinkage	Creep Only$^{\#}$	Creep & shrinkage^{+}
(1)	(2)	(3)	(4)	(5)	(6)	(7)	(8)	(9)
GH	**Left**	7	10.62	11.22	13.66	15.90	21.75	41.71
		14	10.46	10.84	13.25	14.73	22.23	35.89
		21	10.39	10.69	13.03	14.27	21.89	33.49
	Right	7	100.67	95.17	98.26	153.07	3.25	60.84
		14	100.63	96.84	99.12	144.02	2.35	48.72
		21	100.62	97.61	99.50	140.50	1.94	43.94
HI	**Left**	7	98.20	92.88	95.22	144.36	2.52	55.43
		14	98.21	94.51	96.09	136.44	1.67	44.37
		21	98.21	95.25	96.50	133.38	1.31	40.03
	Right	7	78.75	78.57	79.03	122.67	0.59	56.13
		14	78.74	79.15	79.31	114.47	0.20	44.62
		21	78.73	79.26	79.36	111.14	0.13	40.22
IJ	**Left**	7	79.42	79.08	79.77	122.51	0.87	54.92
		14	79.40	79.67	80.04	114.51	0.46	43.73
		21	79.38	79.79	80.09	111.27	0.38	39.45

$^{\#}$100 [column (6)-column (5)]/column (5) $^{+}$100 [column (7)-column (5)]/column (5)

3.1.1 Effect of Concrete age at time of loading

Three ages at loading (t_1=7 days, 14 days and 21 days) are considered. The concrete is assumed to be cured for 7 days i.e. t_s=7 days . The other data chosen is: w=20.00kN/m; f_{ck}=30N/mm^2 and RH=70%. The load, w includes self-weight, superimposed dead load and the portion of the live load which is permanent in nature. The time-dependent analysis is carried out considering creep only and considering both creep and shrinkage. For t_1=7 days, 14 days and 21 days, the values of creep coefficient ϕ at time t_{21} for age of loading t_1 i.e. $\phi(t_{21}, t_1)$ are obtained as 2.50, 2.36 and 2.26 respectively and the values of shrinkage strain ε^{sh} for the time duration t_1 to t_{21} i.e. $\varepsilon^{sh}(t_{21}, t_1)$ are obtained as 437.0×10^{-6}, 356.2×10^{-6} and 324.62×10^{-6} respectively. It may be noted that there is a more pronounced effect of t_1 on the shrinkage strain $\varepsilon^{sh}(t_{21}, t_1)$ than on the creep coefficient $\phi(t_{21}, t_1)$.

The effect of age at loading on instantaneous inelastic (considering cracking) bending moment $M^{it}(t_1)$ and total bending moment $M^t(t_{21})$ at ends of beams GH, HI and IJ only (noting the symmetry of the frame) is shown in Table 1.

It is seen that, as expected, changes due to cracking, in elastic $M^{it}(t_1)$ are smaller for higher age of loading; this results from less cracking due to high tensile strength at greater age of loading. It is also observed from Table 1 that the effect of shrinkage is generally much more

Table 2: Effect of age at loading on instantaneous and total midspan deflections of beams of frame EF1 for w=20.00 kN/m, f_{ck}=30N/mm^{2}and RH=70%

Beam	Age (Days)	Midspan deflection (mm)				Time-dependent % change	
		Instantaneous, $d^{it}(t_1)$		Total, $d^t(t_{21})$			
		Elastic (No Cracking)	Inelastic (Cracking)	Creep only	Creep & shrinkage	Creep Only#	Creep & shrinkage+
(1)	(2)	(3)	(4)	(5)	(6)	(7)	(8)
GH	7	3.31	3.47	4.69	6.38	35.16	83.86
	14	3.26	3.38	4.50	5.77	33.14	70.71
	21	3.24	3.33	4.40	5.52	32.13	65.77
HI	7	0.99	1.17	1.56	1.41	33.33	20.51
	14	0.97	1.08	1.45	1.27	34.26	17.59
	21	0.97	1.05	1.40	1.21	33.33	15.24
IJ	7	1.63	1.65	2.32	2.53	40.61	53.33
	14	1.61	1.59	2.20	2.33	38.36	46.54
	21	1.59	1.57	2.15	2.26	36.94	43.95

#100 [column (5)-column (4)]/column (4) +100 [column (6)-column (4)]/column (4)

significant than the effect of creep on the time-dependent changes in inelastic $M^{it}(t_1)$ (e.g. at right end of beam GH, the percentage change due to creep only and both creep and shrinkage are 3% and 61% respectively for t_1 =7 days). Further, it is observed that there is a significant effect of t_1 on the time-dependent percentage changes, due to creep and shrinkage, in inelastic $M^{it}(t_1)$; these changes at right end of beam GH being 61% and 44% for t_1 = 7 days and 21 days respectively. The significant effect owes to the pronounced effect of t_1 on $\varepsilon^{sh}(t_{21}, t_1)$ (as stated earlier).

The effect of t_1, on elastic $d^{it}(t_1)$, inelastic $d^{it}(t_1)$ and $d^t(t_{21})$ for beams GH, HI and IJ is shown in Table 2. All the deflections are with respect to the chord line joining the two ends of a beam.

Again, as for elastic $M^{it}(t_1)$, changes due to cracking in elastic $d^{it}(t_1)$ are smaller for higher age of loading. It is observed that generally both creep and shrinkage contribute significantly to the time-dependent changes in inelastic $d^{it}(t_1)$. Again, there is a significant effect of t_1 on the changes, due to creep and shrinkage, in inelastic $d^{it}(t_1)$; these changes for t_1=7 days, 14 days and 21 days being about 84%, 71% and 66% respectively for beam with highest elastic $d^{it}(t_1)$ (beam GH). As stated earlier, this owes to the pronounced effect of t_1 on $\varepsilon^{sh}(t_{21}, t_1)$.

In accordance with the observed higher instantaneous deflection of the exterior span than interior spans, the time-dependent changes are also higher for exterior spans.

Consider also, two cast in situ two-span continuous composite beams EB2 and EB3 (length of each span =5.8 m) for which the experimental results were reported by Gilbert and Bradford [13] for 340 days (ϕ =1.68, ε^{sh} =0.00052). The cross-section of the composite beams consisted of a steel section (203×133 UB 25) and a concrete slab of dimensions 1000 mm× 70 mm with a reinforcement of area 213 mm^2 placed at a distance of 15 mm from the top fiber. The

properties of concrete at 28 days were: modulus of elasticity of concrete, E_c=22000 N/mm^2; tensile strength, f_t = 3.0 N/mm^2 and modulus of elasticity of steel, E_s=2 $\times$ 10^{5}N/mm^2. The beam EB2 was subjected to a load, w =6.67 kN/m whereas beam EB3 was subjected to w =1.92 kN/m.

For the present study, the beams EB2 and EB3 have been modeled as a limiting case of a two bay single story frame having one hinge support and two roller supports. The columns of the frame are assumed to have a large area, negligible moment of inertia and negligible length. The concrete age at time of loading (age at loading) of the beams has not been specified by Gilbert and Bradford [13], therefore two ages at loading i.e values of t_1 =3 days and 7 days are considered. Further, since in this case, the creep coefficient and shrinkage strains are already reported (ϕ =1.68 and ε^{sh} =0.00052), only their variation with time is assumed to vary in accordance with CEB-FIP MC 90-99. The construction is assumed to be of propped type and beams are assumed to be loaded as soon as props are removed and thus the load is resisted by the composite section. It may be noted that in the continuous composite beams with the cast in situ concrete and propped construction, the effect of shrinkage, up to the time the props are present, would be negligible if the props are at a sufficiently close spacing. Therefore, such beams would behave in a manner similar to composite beams with precast decks.

Figure 7 presents the midspan deflections of the beams, $d^t(t)$, obtained by the hybrid procedure for t_1 =3 days and 7 days along with the results of the experimental study. It may be noted that the effect of age at loading (t_1) is small on the total midspan deflections. This owes to the fact that the same values of ϕ(=1.68) and ε^{sh}(=0.00052) as reported in the experimental study have been assumed for both the ages of loading. The small difference may be attributed to different magnitudes of instantaneous crack lengths owing to different tensile strengths at the time of application of load.

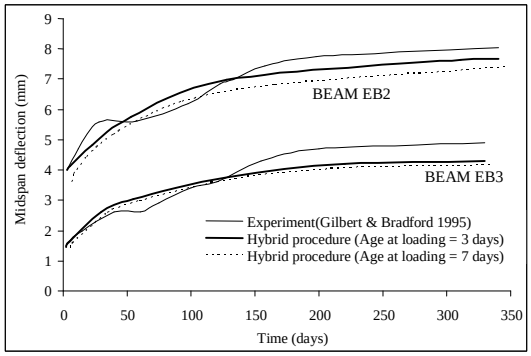

Figure 7: Midspan deflections of beams EB2 and EB3.

3.1.2 Effect of Magnitude of Load

The load w is varied from 10.00 kN/m to 30.00 kN/m. The other data chosen is: t_s= 7 days; t_1=14 days, f_{ck}=30N/mm^2 and RH =70%. For the chosen data, the values of $\phi(t_{21}, t_1)$ and $\varepsilon^{sh}(t_{21}, t_1)$ are obtained as 2.36 and 356.2×10^{-6} respectively. It may be noted that at the time of application of the load, cracking anywhere in the frame is initiated at a load of 15.0 kN/m.

The effect of the magnitude of load on time dependent changes in bending moments is shown in Figure 8. It is seen that magnitude of changes due to creep and shrinkage, in inelastic $M^{it}(t_1)$ for different magnitudes of loading are generally not much different since the changes in bending moment are primarily due to shrinkage which is independent of loading. The percentage changes are though different owing to different values of inelastic $M^{it}(t_1)$, the percentage changes for w=10.00kN/m and 30.00 kN/m being about 79% and 41% respectively at right end of beam HI.

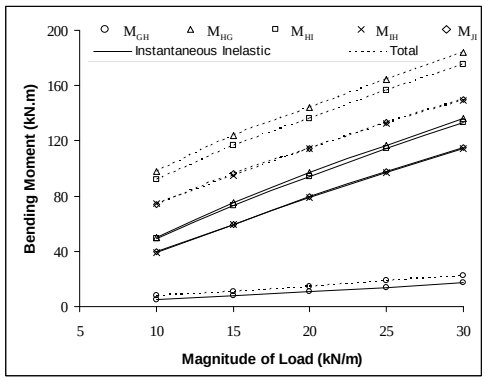

Figure 8: Effect of magnitude of load on instantaneous and total bending moments at ends of beams of frame EF1 for t_1=14 days, and f_{ck}=30N/mm^2 and RH=70%.

Figure 9 shows the effect of magnitude of load on elastic $d^{it}(t_1)$, inelastic $d^{it}(t_1)$ and $d^t(t_{21})$. It is observed that magnitude of changes increase with the magnitude of load. Though, the percentage changes, due to creep and shrinkage, in inelastic $d^{it}(t_1)$ may increase (beam HI) or decrease (beam GH) with the increase in magnitude of loading. Differing magnitudes of crack lengths, and the influence of adjacent beams result in this increase or decrease. An increase in crack length has two opposing effects: (i) increased portion with reduced flexural rigidity tending to increase the midspan deflections and (ii) increased portion with reduced creep and shrinkage tending to reduce the increase in the midspan deflections.

3.1.3 Effect of Grade of Concrete

As stated before, compressive strength of concrete (grade of concrete) has been recognized as one of the significant factors affecting creep and shrinkage of concrete specimens. The grade of concrete is assumed to vary from M 20 to M 40 (f_{ck}=20N/mm^2 to 40N/mm^2). The other data chosen is: w=20.00 kN/m ; t_s= 7 days ; t_1=14 days and RH=70%. For f_{ck}=20N/mm^2

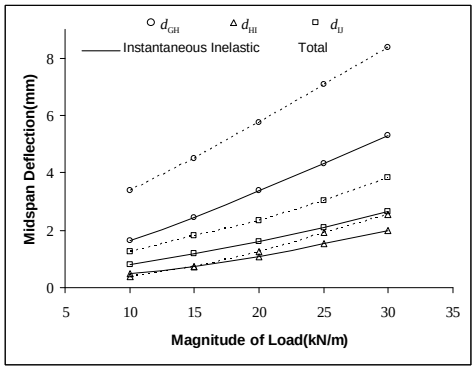

Figure 9: Effect of magnitude of load on instantaneous and total midspan deflections of beams of frame EF1 for t_1=14 days, and f_{ck}=30N/mm^2 and RH=70%.

and 40N/mm^2, the values of $\phi(t_{21}, t_1)$ are 3.20 and 1.88 respectively and those of $\varepsilon^{sh}(t_{21}, t_1)$ are 409.9×10^{-6} and 311.7×10^{-6} respectively.

The effect of grade of concrete on inelastic $M^{it}(t_1)$ and $M^t(t_{21})$ at the ends of beams is shown in Figure 10. It is observed that, inelastic $M^{it}(t_1)$ differ slightly with grade of concrete. The slight difference is owing to different crack lengths resulting from different tensile strengths. Although, as stated above, the compressive strength of concrete is one of the important factors affecting creep and shrinkage of concrete specimens, the percentage change, due to creep and shrinkage, in inelastic $M^{it}(t_1)$ do not differ much with grade of concrete. The maximum percentage change is observed at left end of beam GH (smallest bending moment); the changes for f_{ck}=20N/mm^2 and 40N/mm^2 being about 43%, 31% and 29% respectively. The difference in percentage change for bending moments at other ends which are of design significance is not more than 6%. Although, creep and shrinkage differ significantly with grade of concrete, the corresponding difference is not observed in time-dependent change since it depends additionally on modulus of elasticity of concrete and on crack lengths (as explained earlier).

The effect of grade of concrete on inelastic $d^{it}(t_1)$ and $d^t(t_{21})$ is shown in Figure 11. As expected, inelastic $d^{it}(t_1)$ is higher for lower grade of concrete. The time-dependent percentage change, due to creep and shrinkage, in inelastic $d^{it}(t_1)$ differ slightly with grade of concrete; these changes for f_{ck}=20N/mm^2 and 40N/mm^2 are about 76% and 65% respectively for beam with highest inelastic $d^{it}(t_1)$ (beam GH).

3.1.4 Effect of Relative Humidity

Relative humidity is another factor recognized as one of the significant factors affecting the creep and shrinkage of concrete specimens. The value of relative humidity is varied from 50% to 90%. The other data chosen is: w=20.00 kN/m; t_s=7 days; t_1=14 days; and f_{ck}=30N/mm^2. For RH=50% and 90%, the values of $\phi(t_{21}, t_1)$ are 2.99 and 1.71 respectively and those of $\varepsilon^{sh}(t_{21}, t_1)$ are 474.32×10^{-6} and 146.9×10^{-6} respectively.

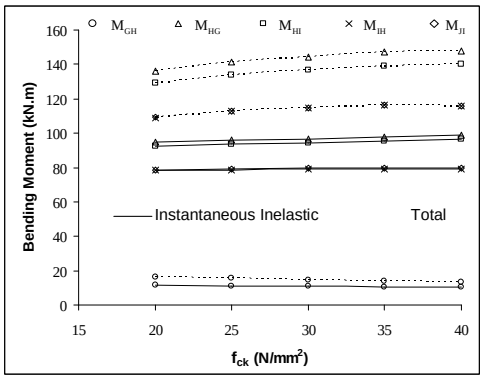

Figure 10: Effect of grade of concrete on instantaneous and total bending moments at ends of beams of frame EF1 for w=20.00kN/m, t_1=14 days, and RH=70%.

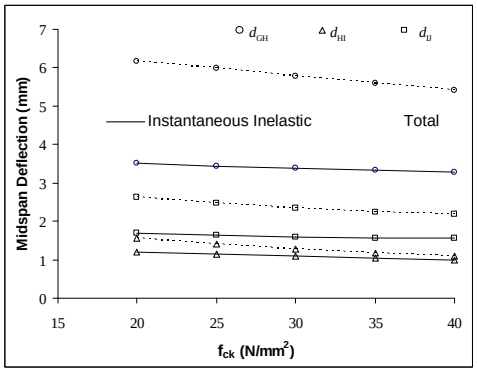

Figure 11: Effect of grade of concrete on instantaneous and total midspan deflections of beams of frame EF1 for w=20.00kN/m, t_1=14 days, and RH=70%.

The effect of relative humidity on $M^t(t_{21})$ at the ends of the beams is shown in Figure 12. There is a significant effect of relative humidity on the time-dependent percentage change, in inelastic $M^{it}(t_1)$. For example, the change varies from about 56% to about 25%, at right end of beam GH, when RH increases from 50% to 90%. This is in accordance with the significant effect of relative humidity observed on creep and shrinkage characteristics of concrete specimens by Howells et al. [15].

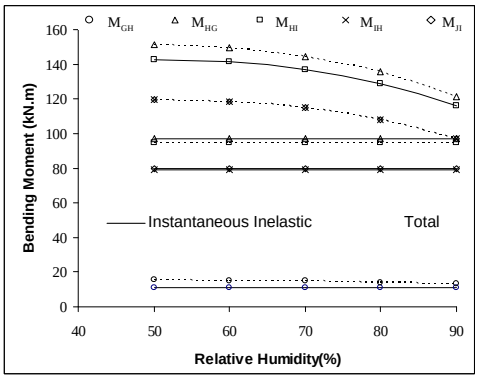

Figure 12: Effect of relative humidity on total bending moments at ends of beams of frame EF1 for w=20.00kN/m, t_1=14 days, and f_{ck}=30N/mm^2

The effect of relative humidity on time-dependent changes in midspan deflections is shown in Figure 13. Again, there is a significant effect of relative humidity on the time-dependent percentage change, in inelastic $d^{it}(t_1)$; the change for beam GH [beam with highest elastic $d^{it}(t_1)$] being about 84% and 44% respectively for RH= 50% and 90% respectively.

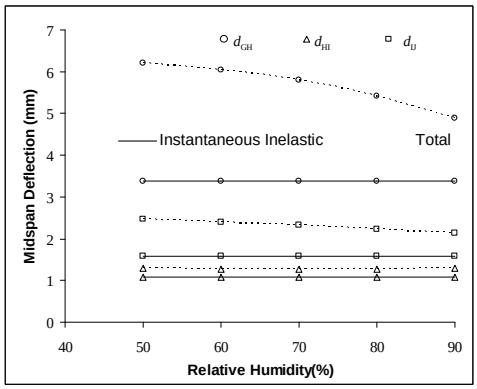

Figure 13: Effect of relative humidity on total midspan deflections of beams of frame EF1 for w=20.00kN/m, t_1=14 days, and f_{ck}=30N/mm^2

It is also observed from the Figures, that for low values of RH, the time-dependent changes significantly affect the values of $M^t(t_{21})$ and $d^t_m(t_{21})$.

Table 3: Effect of tension stiffening on instantaneous and total bending moments at ends of beams of frame EF1 for w=20.00kN/m, t_1=14 days, f_{ck}=30N/mm^2 and RH=70%.

Beam	**End**	**Tension Stiffening (TS)**	**Instantaneous Stage,** $t = t_1$			**Time** $t = t_{21}$	
			Elastic Moment (No Cracking)	Inelastic Moment (Cracking)	%Effect of TS	Total $M^t(t_{21})$	%Effect of TS
(1)	(2)	(3)	(4)	(5)	(6)	(7)	(8)
GH	**Left**	Not considered	10.46	11.56	-6.23%	15.57	-5.40%
		Considered	10.46	10.84		14.73	
	Right	Not considered	100.63	90.80	6.65%	135.24	6.49%
		Considered	100.63	96.84		144.02	
HI	**Left**	Not considered	98.21	88.73	6.51%	128.19	6.20%
		Considered	98.21	94.51		136.44	
	Right	Not considered	78.74	77.85	1.67%	111.89	2.31%
		Considered	78.74	79.15		114.47	
IJ	**Left**	Not considered	79.40	78.27	1.79%	111.76	2.47%
		Considered	79.40	79.67		114.51	

3.1.5 Effect of Tension Stiffening

The data chosen is: w=20.00 kN/m; t_s=7 days; t_1=14 days; f_{ck}=30N/mm^2; and RH=70%. For the chosen data, the values of $\phi(t_{21}, t_1)$ and $\varepsilon^{sh}(t_{21}, t_1)$ are obtained as 2.36 and 356.2×10^{-6} respectively.

The effect of tension stiffening on inelastic $M^{it}(t_1)$ and $M^t(t_{21})$ at the ends of the beams is shown in Table 3. From the table it is seen that the effect of tension stiffening is only marginal since the loading (w=20.00 kN/m) is only marginally higher than the cracking load (w=15.00 kN/m). It is also seen from the table that the percentage effect of tension stiffening at $t = t_1$ and $t = t_{21}$ are similar, thus tension stiffening has only a small effect on the time-dependent changes in bending moments due to creep and shrinkage.

The effect of tension stiffening on inelastic $d^{it}(t_1)$ and $d^t(t_{21})$ for beams is shown in Table 4. As expected, higher inelastic $d^{it}(t_1)$ is predicted for all the three beams, when tension stiffening is not considered. Again, as for bending moments, tension stiffening has only a small effect on time-dependent changes in the midspan deflection of the span of design significance (span GH).

3.1.6 Combinations of rheological parameters

Now consider two combinations of extreme values of the parameters in the chosen range for the frame EF1 (w=20.00 kN/m; t_s=7 days). The values of parameters chosen for combination 1 are: t_1=7 days; f_{ck}=20N/mm^2; and RH=50% and for combination 2 are: t_1=21 days; f_{ck}=40N/mm^2; and RH=90%. The values of $\phi(t_{21}, t_1)$ and $\varepsilon^{sh}(t_{21}, t_1)$ are obtained as 4.42 and 669.5×10^{-6} respectively for combination 1, and 1.35 and 117.2×10^{-6} respectively for combination 2.

Table 4: Effect of tension stiffening on instantaneous and total midspan deflections of beams of frame EF1 for w=20.00 kN/m, t_1=14 days, f_{ck}=30N/mm^2 and RH=70%.

Beam	**Tension Stiffening (TS)**	**Instantaneous Stage,** $t = t_1$			**Time** $t = t_{21}$		
		Elastic deflection (No Cracking)	Inelastic deflection (Cracking)	%Effect of TS		Total $d^t(t_{21})$	%Effect of TS
(1)	(2)	(3)	(4)	(5)	(6)	(7)	(8)
GH	Not considered	3.26	3.56	-5.06%		6.05	-4.63%
	Considered	3.26	3.38			5.77	
HI	Not considered	0.97	1.32	-18.2%		1.66	-23.5%
	Considered	0.97	1.08			1.27	
IJ	Not considered	1.61	1.68	-5.36%		2.49	-6.43%
	Considered	1.61	1.59			2.33	

The effect of two combinations on elastic $M^{it}(t_1)$, inelastic $M^{it}(t_1)$ and $M^t(t_{21})$ at the ends of the beams is shown in Table 5. It is observed that the time-dependent percentage change, due to creep and shrinkage, in inelastic $M^{it}(t_1)$ for combination 1 can be more than three times the change for combination 2 (left end of beam GH). The time-dependent changes in bending moments can therefore be significantly reduced by controlling the rheological parameters.

Table 6 shows the effect of two combinations on elastic $d^{it}(t_1)$, inelastic $d^{it}(t_1)$ and $d^t(t_{21})$ of beams GH, HI and IJ. It is observed that the time-dependent percentage change, due to creep and shrinkage, in inelastic $d^{it}(t_1)$ for combination 1 is more than two times the change for combination 2 for all the three beams. Again, as observed for the bending moments, the time-dependent change in midspan deflection can be reduced significantly by controlling the rheological parameters.

3.2 Five Story and Eight Story Frame

Two low rise composite frames of five story (frame EF1) and eight story (frame EF2) are also considered (Figure 5, $L_1 = L_2 = L_3 = L_4 = L_5$ =7.0m). The effect of sequential construction is small for low rise buildings and is therefore neglected. The cross-section of composite beams is assumed to consist of a steel section (356×171UB 67) and precast concrete slabs of cross-section 1100 mm×75 mm with a reinforcement of area 508 mm^2 placed at a distance of 15 mm from the top fiber. The columns of the frame EF2 consist of steel sections 305×171UB 67, 305×171UB 51, 305×165UB 40, 203×133UB 30, 305×102UB 25 for story levels 1 to 5 respectively. Similarly, the columns of the frame EF3 consist of steel sections 457×191UB 89, 457×191UB 89, 356×171UB 67, 356×171UB 67, 305×165UB 46, 254×146UB 37, 254×146UB 37, 406×140UB 39 for story levels 1 to 8 respectively.

Table 5: Effect of rheological parameters on instantaneous and total bending moments at ends of beams of frame EF1 for w=20.00 kN/m.

Beam	**End**	**Combination**	**Bending Moment (kNm)**			**Time-dependent %change**
			Instantaneous, $M^{it}(t_1)$ Elastic (No Cracking)	Inelastic (Cracking)	**Total,** $M^t(t_{21})$	
(1)	(2)	(3)	(4)	(5)	(6)	(7)
GH	**Left**	1	10.86	11.75	18.88	60.68
		2	10.23	10.34	12.14	17.41
	Right	1	100.72	93.07	150.88	62.11
		2	100.58	99.37	121.01	21.78
HI	**Left**	1	98.20	90.87	141.82	56.07
		2	98.21	97.03	116.28	19.84
	Right	1	78.78	77.42	120.73	55.94
		2	78.71	78.98	94.80	20.03
IJ	**Left**	1	79.46	77.96	120.77	54.91
		2	79.36	79.57	95.22	19.67

Table 6: Effect of rheological parameters on instantaneous and total midspan deflections of beams of frame EF1 for w=20.00 kN/m.

Beam	**Combination**	**Bending Moment (kNm)**			**Time-dependent %change**
		Instantaneous, $d^{it}(t_1)$ Elastic (No Cracking)	Inelastic (Cracking)	**Total,** $d^t(t_{21})$	
(1)	(2)	(3)	(4)	(5)	(6)
GH	1	3.39	3.61	7.29	101.94
	2	3.19	3.22	4.43	37.58
HI	1	1.02	1.30	1.77	36.15
	2	0.95	0.98	1.12	14.29
IJ	1	1.67	1.77	3.03	71.19
	2	1.57	1.55	1.99	28.39

The data chosen is: t_1=14.00 days; w=20.00 kN/m; f_{ck}=30N/mm^2 and RH=70%. For the chosen data, the values of $\phi(t_{21}, t_1)$ and $\varepsilon^{sh}(t_{21}, t_1)$are 2.36 and 356.2×10^{-6} respectively. The behavior is studied at all the floor levels for frame EF2 and some typical floor levels for frame EF3.

The percentage change in bending moments due to creep and shrinkage at beam ends at different floor levels for frames EF2 and EF3 are shown in Figures 14 and 15 respectively. It is observed for these frames that the behavior of first floor is different from the behavior of other floors. This owes to significant lateral displacement, arising from shrinkage, at the ends of first storey columns (foundation being fixed) as compared to negligible differential lateral displacement of columns of other storeys. The use of conventional simplified models like substitute frames (comprising of floor beams and columns above and below the floor) can therefore lead to error in prediction of service load behavior of composite frames.

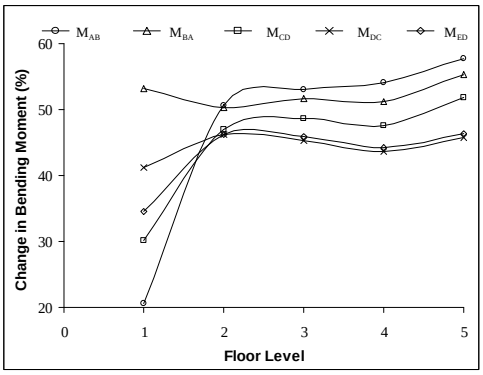

Figure 14: Time-dependent change in bending moments at ends of beams of frame EF2 for w=20.00kN/m, t_1=14 days, and f_{ck}=30N/mm^2 and RH=70%

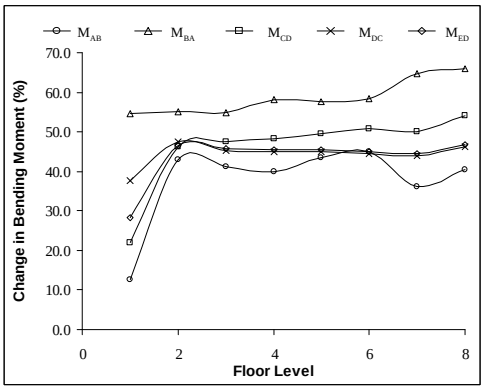

Figure 15: Time-dependent change in bending moments at ends of beams of frame EF3 for w=20.00kN/m, t_1=14 days, and f_{ck}=30N/mm^2 and RH=70%

Figures 16 and 17 show the percentage change in midspan deflections at different floor levels for frames EF2 and EF3 respectively. It is observed that the percentage change in exterior spans is significantly higher than other beams at all the floor levels. Similar behavior has been reported above for frame EF1.

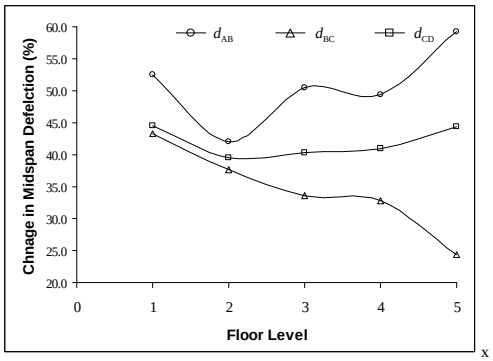

Figure 16: Time-dependent change in midspan deflections of beams of frame EF2 for w=20.00kN/m, t_1=14 days, and f_{ck}=30N/mm^2 and RH=70%

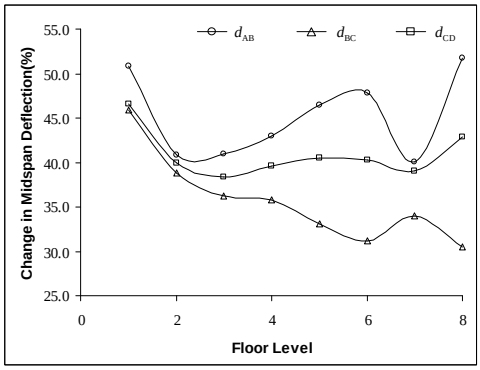

Figure 17: Time-dependent change in midspan deflections of beams of frame EF3 for w=20.00kN/m, t_1=14 days, and f_{ck}=30N/mm^2 and RH=70%

4 Conclusions

The applicability of the hybrid procedure for composite beams with precast decks has been established. It is also shown that cracking of transverse joints has negligible effect on the behavior of composite beams with precsast slabs. Systematic studies are then carried out for the service load behavior of composite frames using the hybrid procedure. For a single story frame, the effect of individual parameters, i.e. t_1, w, f_{ck}, RH and tension stiffening has been

studied on the bending moments and the midspan deflections of beams. Also, for typical values of the parameters, studies have been carried out for a uniform five story and a uniform eight story frame. From the studies, following conclusions are drawn:

- The time-dependent changes in inelastic instantaneous moments at the beam ends are primarily due to shrinkage whereas the time-dependent changes in midspan deflections are due to both creep and shrinkage.
- The relative humidity has a significant effect on the time-dependent changes, in bending moments at the beam ends and midspan deflections.
- The time-dependent changes, in bending moments at supports and midspan deflections, can vary very significantly depending on the combination of rheological parameters. The time-dependent changes can therefore be reduced significantly by controlling the rheological parameters.
- For low rise frames, the order of time-dependent changes in bending moments in beams at first floor level is different from the order of change at other floor levels and it therefore follows that the use of simplified models (substitute frames) can lead to errors.

References

[1] Z. P. Bazant. Prediction of concrete creep effects using age-adjusted effective modulus method. ACI Journal, 69(4):212–217, 1972.

[2] CEB-FIP, editor. model code 1990 for concrete structures. Comité Euro International du Beton-Fédération International de la Précontrainte, Laussane (Switzerland), 1993. Bulletin d information No. 213/214.

[3] S. Chaudhary. Development of a hybrid analytical-numerical procedure and neural networks for composite structures subjected to service load. PhD thesis, Indian Institute of Technology Delhi, New Delhi, India, 2006. PhD thesis.

[4] S. Chaudhary, U. Pendharkar, and A. K. Nagpal. An analytical-numerical procedure for cracking and time-dependent effects in continuous composite beams under service load. Steel and Composite Structures, 7(3):219–240, 2007.

[5] S. Chaudhary, U. Pendharkar, and A. K. Nagpal. A hybrid procedure for cracking and time-dependent effects in composite frames at service load. Journal of Structural Engineering, 133(2):166–175, 2007.

[6] S. Chaudhary, U. Pendharkar, and A. K. Nagpal. A hybrid procedure for cracking, creep, shrinkage and thermal gradient in continuous composite bridges. Latin American Journal of Solids and Structures, 4(3):203–277, 2007.

[7] L. Dezi and A. M. Tarantino. Creep in composite continuous beams. ii: Parametric study. Journal of Structural Engineering, ASCE, 119(7):2112–2133, 1993.

[8] European Committee for Standardization. Eurocode 2: Design of Concrete Structures, Part 1: General rules and rules for buildings. Brussels, Belgium, 1992.

[9] European Committee for Standardization. Eurocode4: Design of composite steel and concrete structures- Part 1: General-Common rules and rules for building. Brussels, Belgium, 2004.

[10] European Committee for Standardization. Eurocode 3: Design of Steel Structures, Part 1: General rules and rules for buildings. Brussels, Belgium, 2005.

[11] Kwak H. G. and Y. J. Seo. Numerical analysis of time-dependent behavior of pre-cast pre-stressed concrete girder bridges. Construction and Building Materials, 16(1):49–63, 2002.

[12] A. Ghali, R. Favre, and M. Elbadry. Concrete Structures: Stresses and Deformations. Spon Press, London, 2002.

[13] R. I. Gilbert and M. A. Bradford. Time-dependent behavior of continuous composite beams at service loads. Journal of Structural Engineering, 121(2):319–327, 1995.

[14] F. Giussani, F. Mola, and A. Palermo. Continuity effects in composite steel-concrete railway bridges. In Proceedings of 6th Int. Conf. Maintenance and Renewal of Permanent Way; Power and Signalling; Structures and Earthworks, London, 2003.

[15] R. W. Howells, R. J. Lark, and B. I. G. Barr. A sensitivity study of parameters used in shrinkage and creep prediction models. Magazine of Concrete Research, 57(10):589–602, 2005.

[16] Fédération internationale du béton. Structural concrete-Textbook on behaviour, design and performance Updated knowledge of the CEB/FIP Model Code 1990. FIB Bulletin 2, Lausane(Switzerland), 1999.

[17] H. G. Kwak and Y. J. Seo. Long-term behavior of composite girder bridges. Computers and Structures, 74(5):583–599, 2000.

[18] A. Mari E. Mirambell and I. Estrada. Effect of construction process and slab prestressing on the serviceability behavior of composite bridges. Journal of Constructional Steel Research, 59(2):135–163, 2003.

[19] G. Ranzi. Short- and long-term analyses of composite beams with partial interaction stiffened by a longitudinal plate. Steel and Composite Structures, 6(3):237–255, 2006.

[20] M. Rutner. The long term tension stiffening in composite bridge construction. Technical Report Rep. No. 8/2003, Dept. of Civil Engineering, Technical University, Munich, Germany, 2003.

[21] H. K. Ryu, S. P. Chang, Y. J. Kim, and B. S. Kim. Crack control of a steel and concrete composite plate girder with prefabricated slabs under hogging moments. Engineering Structures, 27(11):1613–1624, 2005.

[22] Y. J. Seo and H. G. Kwak. Shrinkage cracking at interior supports of continuous pre-cast pre-stressed concrete girder bridges. Construction and Building Materials, 16(1):35–47, 2002.

[23] F. Virtuoso and R. Vieira. Time dependent behavior of continuous composite beams with flexible connection. Journal of Constructional Steel Research, 60(3):451–463, 2004.